Real-time On and Off Road GPS Tracking

Brandon Willard

March 8, 2013
Updated: April 22, 2014

arXiv:1303.1883v2 [stat.AP] 19 Apr 2014

Real-time On and Off Road GPS Tracking

Brandon Willard

March 8, 2013
Updated: April 22, 2014

arXiv:1303.1883v2 [stat.AP] 19 Apr 2014

Abstract

This document describes a GPS-based tracking model for position and velocity states on and off of a road network and it enables parallel, online learning of state-dependent parameters, such as GPS error, acceleration error, and road transition probabilities. More specifically, the conditionally linear tracking model of [Ulmke and Koch (2006)] is adapted to the Particle Learning framework of [H. F. Lopes, et. al.(2011)], which provides a foundation for further hierarchical Bayesian extensions. The filter is shown to perform well on a real city road network while sufficiently estimating on and off road transition probabilities. The model in this paper is also backed by an open-source Java project.

Keywords. Vehicle Tracking, GPS, Particle Filtering, Particle Learning

1 Introduction

The availability and ease of collecting GPS data have created a rising interest in "location aware" applications, many of which define unobservable states such as transportation modes (e.g. walking, biking, driving, etc.), traveled roads, and a users location/velocity relative to streets, sidewalks or landmarks. Real-time GPS data is also being used in trip planning and to ascertain traffic conditions, which involve similar states and modes.

Although the GPS accuracy provided by standard devices may be sufficient for direct use in some simple applications, when one wants to perform inference at lower sampling frequencies, or wants to model some underlying discrete state, more is needed. For example, when dealing with road networks, there are common cases in which "snapping" (orthogonally projecting a GPS point onto a street) is not sufficient in itself. Often, one needs to at least smooth the resulting sequence of snapped road segments in order to get reasonable or coherent results.

Additionally, given the growing use of community sourced maps, such as OpenStreetMap, there is an complementary interest in studying the quality of data. It is possible to ascertain this value by how well the observed data obey the restrictions implicit in the street data. Using a model that includes on/off-road states, one can identify and inspect high off-road likelihood data, which can signify problem areas.

Other use cases for sequential Bayesian estimation involve tracking multiple vehicles with varying properties, such that it may be very difficult to batch estimate parameter values over historical data, but where it is possible to define reasonable limits for the parameter values. For a system that runs day-to-day and adds or removes sources of observations regularly (or, similarly, has unreliable sources), adjustable, sequential parameter learning may be the best option. Generally, when data needs to be removed or augmented real-time, a Bayesian model can easily provide a coherent framework for such actions.

This paper provides an extensible Bayesian model and an efficient particle filter for the estimation of its states and parameters through the Particle Learning (PL) framework. We establish a conditional dynamic linear model (DLM) for on and off-road motion states, and detail the PL estimation procedure. A method for estimating the on-road/off-road probabilities sequentially is provided, and the model is conditionally amenable to conjugate methods of covariance estimation.

Many of aforementioned concerns and requirements are well met by techniques within the conditional DLM setting of [West and Harrison(1997)], and PL framework provides sequential approximate distributions of any estimated parameters. Commonly, sequential Bayesian applications in this domain, have their parameters estimated beforehand, resort to parameter point estimates (e.g. Expectation Maximization), or linearizing (e.g. Extended Kalman Filters). See [D.B. Work et. al. (2010)] for an example of the latter, and [L. Liao, D. Fox, H. Kautz(2004)] for the former.

In such cases the additional information provided by approximating the full parameter distributions isn't available, and/or a departure from a Bayesian setting is made. Also, many such models do not clearly build off of standard motion models, which in the case of conditional DLM's are easy to extend in a hierarchical fashion. For some examples of possible conditional DLM motion models see [X. Rong Li and Vesselin P. Jilkov].

2   The Model

2.1   Paths and Edges

An edge is defined as

$$\lambda = \{(1 - \delta)\, l_\alpha + \delta\, l_\omega \mid \delta \in [0, 1]\}$$

for start and end coordinates $l_\alpha, l_\omega \in \mathbb{R}^2$, and distance along the edge $\delta \in \mathbb{R}^1$. Our construction follows the definition of segments in [Ulmke and Koch (2006)].

A path is defined as an ordered collection of connected edges $\mathcal{P} = \{\lambda^{(N)}, \dots, \lambda^{(1)}\}$ so that $|\mathcal{P}| = N$. It is possible parameterize locations on the path by the distance traveled along all of the ordered edges, i.e.

$$l(d) = \begin{cases} l_0 + l_1 \frac{d - d_1}{d_1} & 0 \le d \le d_1 \\ l_1 + (l_1 - l_2)\frac{d - d_2}{d_2 - d_1} & d_1 \le d \le d_2 \\ \vdots & \vdots \\ l_{N-1} + (l_{N-1} - l_N)\frac{d - D}{D - d_{N-1}} & d_{N-1} \le d \le D \end{cases} \tag{1}$$

where the distance d_k is given by $d_k = \sum_{j=1}^{k} |l_j - l_{j-1}|$, and $l_0 = 0$.

2.1.1 Evaluated Paths

In what follows, we construct our distributions conditional on a path, $\mathcal{P}$. Naturally, the results of our model will depend very much on the $\mathcal{P}$ we consider and, in application, it is usually impractical to evaluate the entire support of $\mathcal{P}$. Also, it's often clear that the majority of $\mathcal{P}$ will have near zero likelihood, so it's reasonable to employ a technique for finding useful subsets to evaluate, like an efficient sampling procedure or a search algorithm.

The approach used here is to employ a modified A^* search between some measure of the current state and an area around the observation. In the DLM-based motion model one can simply use the observation covariance to determine an area for finding A^* destination nodes. As well, other motion model information can inform the search, such as the projected distance, which can be used as a heuristic.

2.1.2 Edge Transitions

The generalized prior distribution for edges is a transition matrix, where edges, $\lambda^{(l)}$, are interpreted to be a unique integer index and $\lambda^{(l)} = 0$ indicates no edge (i.e. off-road).

$$p(\lambda^{(j)}|\lambda^{(k)}, \mathcal{P}) \propto \begin{cases} \pi_{on} & j \geq k \text{ and } \lambda^{(j)} > 0 \text{ and } \lambda^{(k)} = 0 \\ \pi_{off} & j \geq k \text{ and } \lambda^{(j)} = 0 \text{ and } \lambda^{(k)} > 0 \\ \pi_r^{(j,k)} & j \geq k \text{ and } \lambda^{(j)}, \lambda^{(k)} > 0 \\ \pi_g^{(j,k)} & j \geq k \text{ and } \lambda^{(j)} = \lambda^{(k)} = 0 \\ 0 & \text{otherwise} \end{cases} \tag{2}$$

for connected edges $\lambda^{(j)}, \lambda^{(k)} \in \mathcal{P}$ and constants $\pi_{on}, \pi_{off}, \pi_r^{(j,k)}, \pi_g^{(j,k)}$. Basically, we've defined a simple on-off and between-edge transition matrix, for which it is straightforward to assign Beta/Dirichlet prior transition probabilities.

Although we assume a simpler on-off only transition distribution in what follows, resulting in a pair of Beta-Bernoulli, the transition matrix formulation makes clear the fact that we can extend this further to cover all road transitions.

2.2 Motion Model

In what follows we specify the probability of assignments to edges in a path, motion along an edge and free movement.

Given an edge $\lambda > 0$, we track the distance traveled and velocity along the edges in $\mathcal{P}$. We define the *road-movement* state vector as

$$x_i^r = \begin{pmatrix} d_i \\ v_i \end{pmatrix}$$

To convert between this vector of road-movement measures and a state vector of 2D coordinates and 2D velocity, called *ground-movement* coordinates, one can use the transform

$$P_1^\lambda = \frac{l_{\alpha(\lambda)} - l_{\omega(\lambda)}}{d_{\omega(\lambda)} - d_{\alpha(\lambda)}}, \quad s_1^\lambda = l_{\alpha(\lambda)} - P_1^\lambda d_{\omega(\lambda)}$$

$$P^\lambda = U(I_2 \otimes P_1^\lambda), s^\lambda = U \begin{pmatrix} s_1^\lambda \\ \mathbf{0} \end{pmatrix}, U = \begin{pmatrix} 1 & 0 & 0 & 0 \\ 0 & 0 & 1 & 0 \\ 0 & 1 & 0 & 0 \\ 0 & 0 & 0 & 1 \end{pmatrix}$$

where $\alpha(\lambda), \omega(\lambda)$ are indicate the start and end distances and positions on λ, and $\mathbf{0} = [0,0]^T$, so that

$$\begin{pmatrix} l_{1,i} \\ v_{1,i} \\ l_{2,i} \\ v_{2,i} \end{pmatrix} = P^\lambda x_i^r + s^\lambda$$

An inverse mapping is $d = P^{\lambda,T}(x - s^\lambda)$ for $x \in \mathbb{R}^4$.

Since the projection does not preserve the magnitude of velocity when going on-road, it is possible that using this transform will have undesired effects in practice. For instance, projecting onto an edge corresponding to a sharp turn could completely diminish the resulting magnitude of velocity. However, one can simply preserve the magnitude of velocity when projecting on-road, or specify another mechanism for altering the resulting velocity of a projection, if desired.

The transition equations and distribution

$$x_{i+1}^r = G_r x_i^r + \Gamma_1 \epsilon_{r,i+1}, \ \epsilon_{r,i+1} \sim N(0, \sigma_r^2) \tag{3}$$

$$G_r = \begin{pmatrix} 1 & \Delta t_i \\ 0 & 1 \end{pmatrix}, \ \Gamma_r = \begin{pmatrix} \frac{\Delta t_i^2}{2} \\ \Delta t_i \end{pmatrix}$$

$$Var[x_{i+1}^r] \equiv W_{i+1}^r = \Gamma_r \Gamma_r^T \sigma_r^2$$

For movement not on a path (i.e. $\lambda = 0$), or when referring to ground-movement coordinates, we switch to a standard planar position-velocity model with

$$x_{i+1}^g = G_g x_i + \Gamma_2 \epsilon_{g,i+1}, \ \epsilon_{g,i+1} \sim N(0, \sigma_g^2 I_2) \tag{4}$$

$$x_i^g = (l_{1,i}, v_{1,i}, l_{2,i}, v_{2,i})^T, \ G_g = I_2 \otimes G_r, \ \Gamma_g = I_2 \otimes \Gamma_r$$

$$Var[x_{i+1}^g] \equiv W_{i+1}^g = \Gamma_g \Gamma_g^T \sigma_g^2$$

All together, we have

$$x_i = \begin{cases} P^\lambda x_i^r + s^\lambda & \lambda > 0 \\ x_i^g & \lambda = 0 \end{cases}$$

4

To summarize, we have two states, x_i^r, x_i^g, straight-line kinematics over a path and free-movement, respectively, then we constructed a general motion state x_i, which projects the path kinematics to ground-coordinates when appropriate.

Finally, with our generalized motion state, the observation equation is

$$y_i = O_g x_i + \epsilon_{y,i}$$

$$O_g^T = \begin{pmatrix} 1 & 0 \\ 0 & 0 \\ 0 & 1 \\ 0 & 0 \end{pmatrix}, \epsilon_{y,i} \sim N(0, \sigma_y^2 I_2)$$

2.2.1 Observation and State Covariance Distributions

A reasonable and effective simplification is to take $\sigma_x \equiv \sigma_r = \sigma_g$ and specify the following conjugate priors

$$\sigma_x^2 \sim IG(\alpha_{x,i}/2, \beta_{x,i}/2)$$
$$\sigma_y^2 \sim IG(\alpha_{y,i}/2, \beta_{y,i}/2)$$

where $IG(\alpha, \beta)$ specifies an Inverse-Gamma distribution with shape and scale parameters, respectively. Like the dynamic factor model example of [H. F. Lopes, et. al.(2011)], we can track the sufficient statistics $\alpha_x, \beta_x, \alpha_y, \beta_y$ through the conditional conjugacy induced after sampling $(x_i, x_{i-1}|y_i, \lambda_i, \sigma_x, \sigma_y)$. The posterior sufficient statistics are given by

$$\begin{align} \alpha_{x,i} &= \alpha_{x,i-1} + 1 \\ \beta_{x,i} &= \beta_{x,i-1} + (x_i - G_{\lambda_i} x_{i-1})^T (\Gamma_{\lambda_i} \Gamma_{\lambda_i}^T)^{-1} (x_i - G_{\lambda_i} x_{i-1}) \\ \alpha_{y,i} &= \alpha_{y,i-1} + 1 \\ \beta_{y,i} &= \beta_{y,i-1} + (y_i - O_g x_i^g)^T (y_i - O_g x_i^g) \end{align} \tag{5}$$

G_{λ_i} signifies whichever state λ_i is associated with: G_r or G_g.

2.2.2 Path Predictions and Posteriors

We proceed to define the predictive distribution for a path $\mathcal{P}$, and then the filter updates. In what follows, path $\mathcal{P}$ always starts with the previous edge λ_i. Also, we define Z_i to be the collection of observations and distribution parameters up to observation i, i.e. $Z_i \equiv \{y_i, \mathcal{K}_i, \lambda_i, \sigma_x, \sigma_y, (\alpha_{x,i}, \beta_{x,i}), (\alpha_{y,i}, \beta_{y,i})\}$ where $\mathcal{K}_i$ are the Kalman filter parameters in ground coordinates $\mathcal{K}_i \equiv \{m_i, C_i\}$.

First, let the road-movement prior predictive distribution be

$$p\left(x_{i+1}^r | Z_i\right) \sim N(\tilde{a}_{i+1}, \tilde{R}_{i+1})$$

which we obtain from (3). The use of tildes on the mean and variance parameters signify road-coordinates.

A straight-forward construction of the predictive distribution for a given path would involve strictly assigning the edge that corresponds to the predicted length, as in

$$p(x_{i+1}^r, \lambda_{i+1}|\mathcal{P}, Z_i) = p\left(x_{i+1}^r|Z_i\right) p\left(\lambda_{i+1}|x_{i+1}^r, \mathcal{P}\right) p(\lambda_{i+1}|\lambda_i, \mathcal{P}) \tag{6}$$

$$p(\lambda_{i+1}|x_{i+1}^r, \mathcal{P}) \propto \begin{cases} 1 & O_r x_{i+1}^r \in [d_{\alpha(\lambda_{i+1})}, d_{\omega(\lambda_{i+1})}] \\ 0 & \text{otherwise} \end{cases} \tag{7}$$

where $O_r = (1, 0)$. Basically, we want to truncate the state distribution so that it lies strictly on the given edge; however, such a distribution would forfeit the simple conditional linearity and conjugacy, so we resort to a rather effective approximation. Following [Ulmke and Koch (2006)], we replace the step function in (7) by a normal distribution centered on the edge and with a variance proportional to its length,

$$p\left(\lambda_{i+1}|x_{i+1}^r, \mathcal{P}\right) \propto f_N\left(\bar{d}_{\lambda_{i+1}}; O_r x_{t+1}^r, \Delta d_{\lambda_{i+1}}^2\right) \tag{8}$$

where

$$\bar{d}_\lambda = (d_{\omega(\lambda)} + d_{\alpha(\lambda)})/2, \ \Delta d_\lambda = (d_{\omega(\lambda)} - d_{\alpha(\lambda)})/\sqrt{12}$$

It is important to recall that the distance terms $\bar{d}_\lambda, \Delta d_\lambda, d_{\omega(\lambda)}, d_{\alpha(\lambda)}$ are path dependent, such that $d_{\alpha(\lambda)}$ is the distance up to the start of λ on $\mathcal{P}$.

Moving on, we can derive a categorical prior predictive distribution over $\lambda_{i+1} \in \mathcal{P}$ using (6)

$$p\left(\lambda_{i+1}|\mathcal{P}, Z_i\right) \propto f_N(\bar{d}_{\lambda_{i+1}}; O_r \tilde{a}_{i+1}, O_r \tilde{R}_{i+1} O_r^T + \Delta d_{\lambda_{i+1}}^2)$$

From here we can solve the prior prediction equations, in road-movement coordinates, for one edge with

$$p\left(x_{i+1}^r|\lambda_{i+1}, \mathcal{P}, Z_i\right) \propto p\left(\lambda_{i+1}|x_{i+1}^r, \mathcal{P}\right) p\left(x_{i+1}^r|Z_i\right)$$

so that

$$p\left(x_{i+1}^r|\lambda_{i+1}, \mathcal{P}, Z_i\right) \sim N\left(\tilde{a}_{i+1}^\lambda, \tilde{R}_{i+1}^\lambda\right)$$

and, as in [Ulmke and Koch (2006)]

$$\begin{aligned} \tilde{a}_{i+1}^\lambda &= \tilde{a}_i + W_{i+1}^\lambda\left(\bar{d}_\lambda - O_r \tilde{a}_i\right), & \tilde{R}_{i+1}^\lambda &= \tilde{R}_{i+1} - W_{i+1}^\lambda S_{i+1}^\lambda W_{i+1}^{\lambda}{}^T \\ W_{i+1}^\lambda &= \tilde{R}_{i+1} O_r^T S_{i+1}^{-1, \lambda}, & S_{i+1}^\lambda &= O_r \tilde{R}_{i+1} O_r^T + \Delta d_\lambda{}^2 \end{aligned}$$

We can now obtain the prior predictive distribution in ground-coordinates

$$p\left(x_{i+1}|\mathcal{P}, Z_i\right) \propto \sum_{\lambda_{i+1} \in \mathcal{P}} p\left(x_{i+1}|\lambda_{i+1}, \mathcal{P}, Z_i\right) p\left(\lambda_{i+1}|\mathcal{P}, Z_i\right) p(\lambda_{i+1}|\lambda_i, \mathcal{P})$$

$$p\left(x_{i+1}|\lambda_{i+1}, \mathcal{P}, Z_i\right) \sim N\left(a_{i+1}^\lambda = P^\lambda \tilde{a}_{i+1}^\lambda + s^\lambda, R_{i+1}^\lambda = P^\lambda \tilde{R}_{i+1}^\lambda P^{\lambda, T}\right)$$

Filtering is accomplished by conversion to ground coordinates, then updating the state sufficient statistics, through normal Kalman filtering

$$p\left(x_{i+1}|\mathcal{P}, Z_{i+1}\right) \propto \sum_{\lambda_{i+1}\in\mathcal{P}} p\left(\lambda_{i+1}|\lambda_i,\mathcal{P},Z_i\right) \int_{x_{i+1}} p\left(y_{i+1}|x_{i+1}\right) p\left(x_{i+1}|\lambda_{i+1},\mathcal{P},Z_i\right)$$
$$\propto \sum_{\lambda_{i+1}\in\mathcal{P}} p\left(\lambda_{i+1}|\lambda_i,\mathcal{P},Z_i\right) p\left(x_{i+1}|\lambda_{i+1},\mathcal{P},Z_{i+1}\right)$$

where

$$p\left(\lambda_{i+1}|\lambda_i,\mathcal{P},Z_i\right) = p\left(\lambda_{i+1}|\mathcal{P},Z_i\right) p(\lambda_{i+1}|\lambda_i,\mathcal{P})$$
$$p\left(x_{i+1}|\lambda,Z_{i+1}\right) \sim N\left(m_{i+1}^{\lambda}, C_{i+1}^{\lambda}\right)$$

with posterior mean and covariance
$$\begin{aligned} m_{i+1}^{\lambda} &= a_{i+1}^{\lambda} + A_{i+1}^{\lambda}(y_{i+1} - e_{i+1}^{\lambda}) \\ C_{i+1}^{-1,\lambda} &= R_{i+1}^{-1,\lambda} + O_g^T O_g / \sigma_y^2 \\ A_{i+1}^{\lambda} &= R_{i+1}^{\lambda} O_g^T Q_{i+1}^{-1,\lambda} \end{aligned} \tag{9}$$

and predictive mean and covariance
$$\begin{aligned} e_{i+1}^{\lambda} &= O_g a_{i+1}^{\lambda} \\ Q_{i+1}^{\lambda} &= O_g R_{i+1}^{\lambda} O_g^T + \sigma_y^2 I_2 \end{aligned}$$

and then conversion back to edge coordinates

$$p\left(x_{i+1}^r|\mathcal{P},Z_{i+1}\right) \propto \sum_{\lambda_{i+1}\in\mathcal{P}} p\left(\lambda_{i+1}|\lambda_i,\mathcal{P},Z_{i+1}\right)$$
$$\times N\left(\tilde{m}_{i+1}^{\lambda} = P^{\lambda,T}(m_{i+1}^{\lambda} - s^{\lambda}),\ \tilde{C}_{i+1}^{\lambda} = P^{\lambda,T} C_{i+1}^{\lambda}\ P^{\lambda}\right)$$

Finally, for off-road movement, filtering is performed in ground coordinates, using the standard Kalman filter updates.

3 Estimation

Since our state, x_i, is a DLM conditional on a path and edge, we are able to use Rao-Blackwellization and sufficient statistics. The likelihoods and posteriors are conditionally known, and we are able to sample directly from them, so the results are perfectly adapted ([Pitt and Shephard (1999)], [H. F. Lopes, et. al.(2011)]). This provides a setting that is well suited for estimating hyper-parameters online, even when their estimation entails sampling and not simply conjugate updates.

Considering the defined distributions, we have a situation very reminiscent of the tracking example in [Jun S. Liu et. al.(2001)], and the dynamic factor model with time-varying loadings in [H. F. Lopes, et. al.(2011)], which includes estimation for observation and state covariances. Through a similar design we attempt to relate

their studied efficiencies and improvements to components of our model. Specifically, [Jun S. Liu et. al.(2001)] demonstrates improvements of mixture Kalman filter (MKF) state estimation over plain SIS or particle filters, and [H. F. Lopes, et. al.(2011)] shows the efficiency of state-transition and variance estimation in the PL setting for a MKF. These results have motivated our use of MKF/PL in what follows.

We follow the CDLM section and switching model example in [H. F. Lopes, et. al.(2011)]. Starting with N particles of $Z_i = \{x_i, \lambda_i, \mathcal{K}_i, \sigma_x, \sigma_y, (\alpha_{x,i}, \beta_{x,i}), (\alpha_{y,i}, \beta_{y,i})\}$ approximating $p(x_i, \lambda_i, \mathcal{K}_i | y_i)$ the particle filter steps are

1. *Re-sampling:* Draw an index $k^j \sim Multi(w_i^{(1)}, \dots, w_i^{(N)})$ with weights

$$w_i^{(j)} \propto p(y_{i+1} | (\mathcal{K}_i, \lambda_i)^{(k^j)})$$

with

$$p(y_{i+1} | \mathcal{K}_i, \lambda_i) = \sum_{\mathcal{P}_{i+1}} \sum_{\lambda_{i+1} \in \mathcal{P}_{i+1}} f_N(y_{i+1}; e_{i+1}^{\lambda_{i+1}}, Q_{i+1}^{\lambda_{i+1}}) \, p(\lambda_{i+1} | \lambda_i, \mathcal{P}_{i+1}, Z_i)$$

2. *Propagating state λ:* Draw $\lambda_{i+1}^{(j)}$ from

$$p(\lambda_{i+1} | (\mathcal{K}_i, \lambda_i, \mathcal{P}_{i+1})^{(k^j)}, y_{i+1}) \propto f_N(y_{i+1}; e_{i+1}^{\lambda_{i+1}}, Q_{i+1}^{\lambda_{i+1}}) \, p(\lambda_{i+1} | \lambda_i, \mathcal{P}_{i+1}, Z_i)$$

3. *Propagating state x_{i+1}:* Draw $x_{i+1}^{(j)}$ from $p(x_{i+1}^{(j)} | \lambda_{i+1}, y_{i+1}, \mathcal{K}_i, \sigma_x, \sigma_y)$

4. *Propagating state sufficient statistics, $\mathcal{K}_{i+1}$:* Perform the Kalman filter recursions described in (9), or, for $\lambda_{i+1} = 0$, the standard Kalman recursions.

5. *Propagating parameter sufficient statistics:* Perform off-line updates for hyper-parameters π_{on}, π_{off} and (5), then draw σ_x, σ_y.

4   Implementation

In what follows we observe the performance of the Particle Learning filter described above against a simple Bootstrap filter. We are primarily concerned with basic accuracy, stability and the computational requirements for runs of decent length over a non-trivial graph. Secondly, through simulation we are able to directly measure the accuracy of parameter estimation. For our implementation we used a graph of Washington DC, and generated roughly 1000 of observations for each run.

The Bootstrap filter estimates only the states, as described below, and the PL filter estimates the states and edge transitions. To do this, the distribution in (2) is partitioned into two Bernoulli distributions with Beta distributed transition probabilities, under the restriction that $\pi_r^{(j,k)} = \pi_r, \pi_g^{(j,k)} = \pi_g$ (the same restriction is used in the simulations and bootstrap filter). Due to conjugacy, updates are straight-forward and performed in step 5 above. This construction follows the transition matrix in Example 3 of [H. F. Lopes, et. al.(2011)].

4.1 Bootstrap Filter and Simulation Procedure

The bootstrap filter (BS) consists of sampling $p(x_{i+1}|x_i, \mathcal{P})$ by first updating per (3) or (4), and including the error due to the state transition covariance. Then, for the case of $\lambda \neq \emptyset$ we move in the direction and length of the sampled movement, sampling edge transitions according to (2) and (7). Simulations are produced in exactly the same way.

Furthermore, when filtering, the effective sample size (ESS) is calculated for the propagated sample set and a condition is checked to determine if resampling is required. The condition was set to $ESS < 0.9N$, where N is the initial sample size.

4.2 Setup

Both models are run on the same simulated data set with varying particle sizes and run lengths. The true parameters were

$$\Delta t = 30$$
$$\sigma_y^2 = 100 \, I_2$$
$$\sigma_r^2 = 6.25 \times 10^{-4}$$
$$\sigma_g^2 = 6.25 \times 10^{-4} I_2$$
$$\pi_g = 0.05, \pi_{on} = 0.95$$
$$\pi_{off} = 0.05, \pi_r = 0.95$$

The BS filter was run using the true parameters as well as the PL filter with the exception of the π parameters, which were replaced by Beta parameters equaling

$$(\alpha_{off,off} = 15, \alpha_{off,on} = 20)$$
$$(\alpha_{on,on} = 70, \alpha_{on,off} = 100)$$

for the "off" and "on" distributions, respectively.

Simulations were performed on an Intel Core i5 with 16 gigs of RAM on Ubuntu 12.01 and using Java 6 OpenJDK amd64, and for each observation the root mean squared error (RMSE) of the position-velocity state vector, in ground-coordinates, was computed over the set of posterior particles.

4.3 Results

Figures 1, 2 compare the log RMSE values for the two filters. Figure 1 shows that PL RMSE is lower, on average, than BS, across all particle sizes, but the most noticeable difference is how many fewer particles PL takes for its accuracy. Figures 4, 3 show 95% credibility intervals for the estimated $\pi_{off,off}, \pi_{on,on}$ with $\sigma_g^2 = 6.25 \times 10^{-3} I_4$ in both the simulations and PL filters.

The online estimation of $\pi_{off,off}, \pi_{on,on}$ demonstrates some of the inherent complexities with having on and off-road states. For example, in Figure 3 we can see that estimation is biased upward in both terms. Observing the data directly, we often find that off-road states are not propagated due to the location in which the simulation goes

off-road. Where there are many streets close together, an off-road state that lasts for one observation is easy to interpret as an on-road state, since there will likely exist connecting roads that fit with the true velocity and location. The same goes for cases in which an off-road state is traveling parallel to or, for all practical purposes, on a road. We would expect that longer off-road sojourn times would help differentiate, e.g. Figure 3, or noticeably different dynamics for off-road states, and they do. The off-road to off-road probability in Figure 3 is very small, so we can expect that staying off-road is very brief, and, given the large size of π_{on}, the simulation doesn't go off-road very often. Figure 4 shows that increasing π_{off} can help identify the signal.

The results were computed in Java, synchronously, and, are naturally implementation dependent. Most of the time spent in the PL filter revolves around an A^* computation of shortest paths. In the implementation used here, some caching was utilized to avoid repeated computations, and, of course, the BS filter does not require such computations. The BS filter is clearly the faster choice for low particle size, but referencing Figures 1, 2 we can see that to achieve an RMSE comparable to the PL filter one needs to increase the particle size, which pulls the BS filter's throughput results to those of the PL filter at 25 particles.

Regarding the filter comparison in generality, we're mostly seeing the documented benefit of using fully-adapted, Rao-Blackwellized filters, since the advantage of path-searching over path-sampling has been mostly diminished. To address this difference, the above tests were performed with parameters that restricted the distances moved between observations to values that do not push the limits of path-searching against sampling. The simulations spend most of their time transitioning between 0-3 edges, so that simple edge sampling is unlikely to fail at finding the true paths.

For models or data with larger state covariances, and thus more error due to acceleration, the comparison between path generating methods may not be useful, as path-sampling models like the BS filter will quickly face issues. The same goes for settings in which the graph is more dense and/or paths are more restricted. In tests, when dead-end's are reached, or highly divergent paths are taken, we've observed that both models will eventually go off-road and find their way back to the correct path (this also accounts for some of the bias in π_{on}, π_{off} estimation). This can be seen in the RMSE results, as in 2, where large values appear in series. Even though the simulation parameters are less likely to cause these events, the city graphs are non-trivial, so the behaviour is present, and, for the times in which it does occur, we can see that with increasing particle size the BS filter is less affected, as expected.

5   Conclusion and Future Work

The results demonstrate that the PL model is effective in this setting, and that it can perform well relative to a standard bootstrap filter based on the exact data generating process for an actual city graph. The simulations were designed to approximate the observed on and off road behaviour of real data collected in Cebu and DC, and the estimation was sufficient for those settings. Generally, outside of the present paper's simulations and in real use cases, the PL filter's MAP results were observed to be overall

accurate at inferring traveled segments and on/off states containing a mix of walking and biking in the DC area. In summary, alongside the know benefits of MKF filtering in a tracking scenario, we can add the ability to infer traveled paths and off-road behaviour in real-time.

Future work could involve demonstrating and studying more of the learning aspects, like covariance estimation, by using more interesting edge transition models, as well as testing the limits of accuracy in varied acceleration settings. Comparisons with other sophisticated or specialized models may be of use in determining comparative advantages in certain scenarios, too. Otherwise, one clear line of investigation involves an analysis of the resulting smoothed paths, since many applications of such a model require accurate edge-to-edge estimation, or even the elucidation of off-road trajectories.

The model is available as an open-source project at `https://github.com/brandonwillard/open-tracking-tools`. The results in this paper were all produced with the aforementioned code, which is setup to filter custom csv data and produce simulations for any city using OpenTripPlanner graphs (`opentripplanner.org`) built with OpenStreetMap (`www.openstreetmap.org`) data.

6   Thanks

I would like to thank Prof. Yali Amit, Mei Wang and Hedibert Lopes for their input and support, and OpenPlans.org for the great community and opportunities to apply this work.

References

[D.B. Work et. al. (2010)] D.B. Work et. al. (2010) "A Traffic Model for Velocity Data Assimilation" Applied Mathematics Research eXpress, Vol. 2010, No. 1, pp. 1-35

[X. Rong Li and Vesselin P. Jilkov] X. Rong Li and Vesselin P. Jilkov (2000) "A Survey of Maneuvering Target Tracking: Dynamic Models" Proceedings of SPIE Conference on Signal and Data Processing of Small Targets, April 2000. (4048-22)

[Jun S. Liu et. al.(2001)] Jun S. Liu, RongChen and Tanya Logvinenko (2001) "A Theoretical Framework for Sequential Importance Sampling and Resampling" Sequential Monte Carlo Methods in Practice, Springer, ?, 2001

[Pitt and Shephard (1999)] Pitt and Shephard (1999) "Filtering via simulation: Auxiliary particle filters." J. Amer. Statist. Assoc. 94, 590-599.

Sequential Monte Carlo Methods in Practice, Springer, ?, 2001

[H. F. Lopes, et. al.(2011)] H. F. Lopes, et. al. (2011) "Particle Learning for Sequential Bayesian Computation" Bayesian Statistics 9, 317–360, 2011

[Ulmke and Koch (2006)] Martin Ulmke and Wolfgang Koch (2006) "Road-Map Assisted Ground Moving Target Tracking" IEEE Transactions on Aerospace and Electronic Systems 4, Vol. 42, 1264-1274, 2006

[H. F. Lopes, et. al.(2011)] H. F. Lopes, et. al. (2011) "Particle Learning for Sequential Bayesian Computation" Bayesian Statistics 9, 317–360, 2011

[West and Harrison(1997)] West, M. and J. Harrison (1997). "Bayesian Forecasting and Dynamic Models"(2nd ed.). Springer Series in Statistics. Springer. 634, 635

[L. Liao, D. Fox, H. Kautz(2004)] L. Liao, D. Fox, and H. Kautz. (2004). "Learning and Inferring Transportation Routines" Proc. of the National Conference on Artificial Intelligence (AAAI-04).
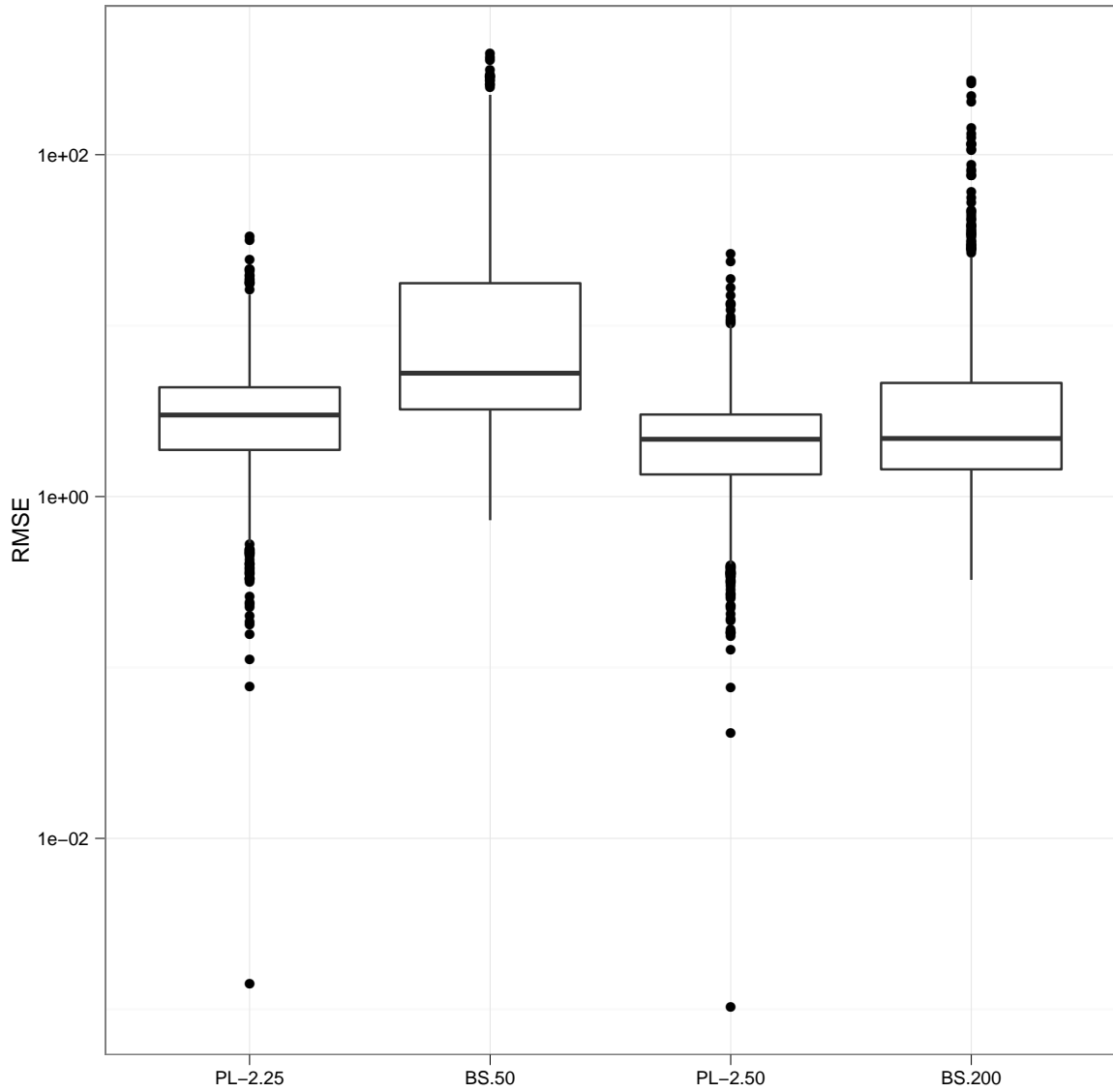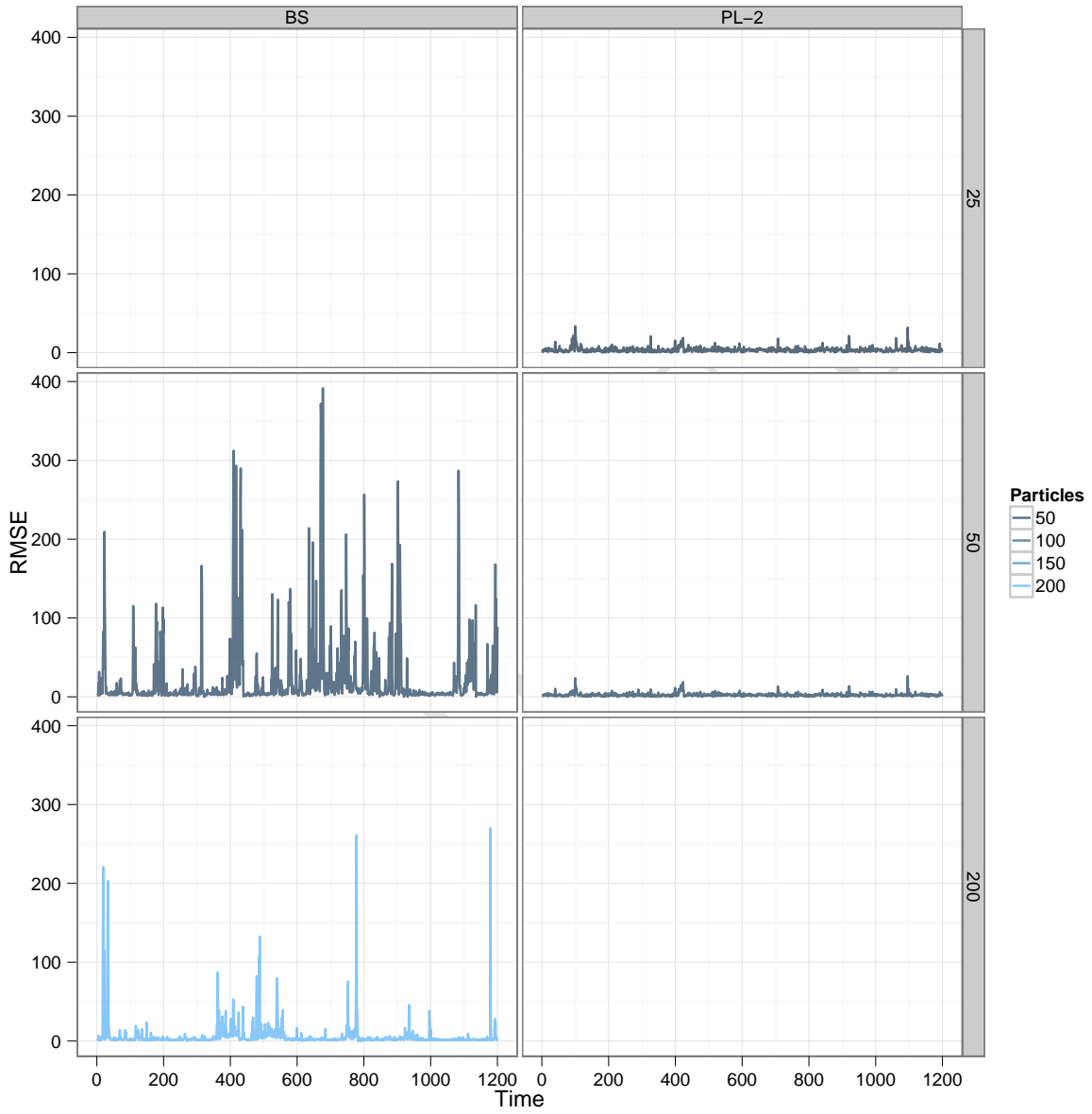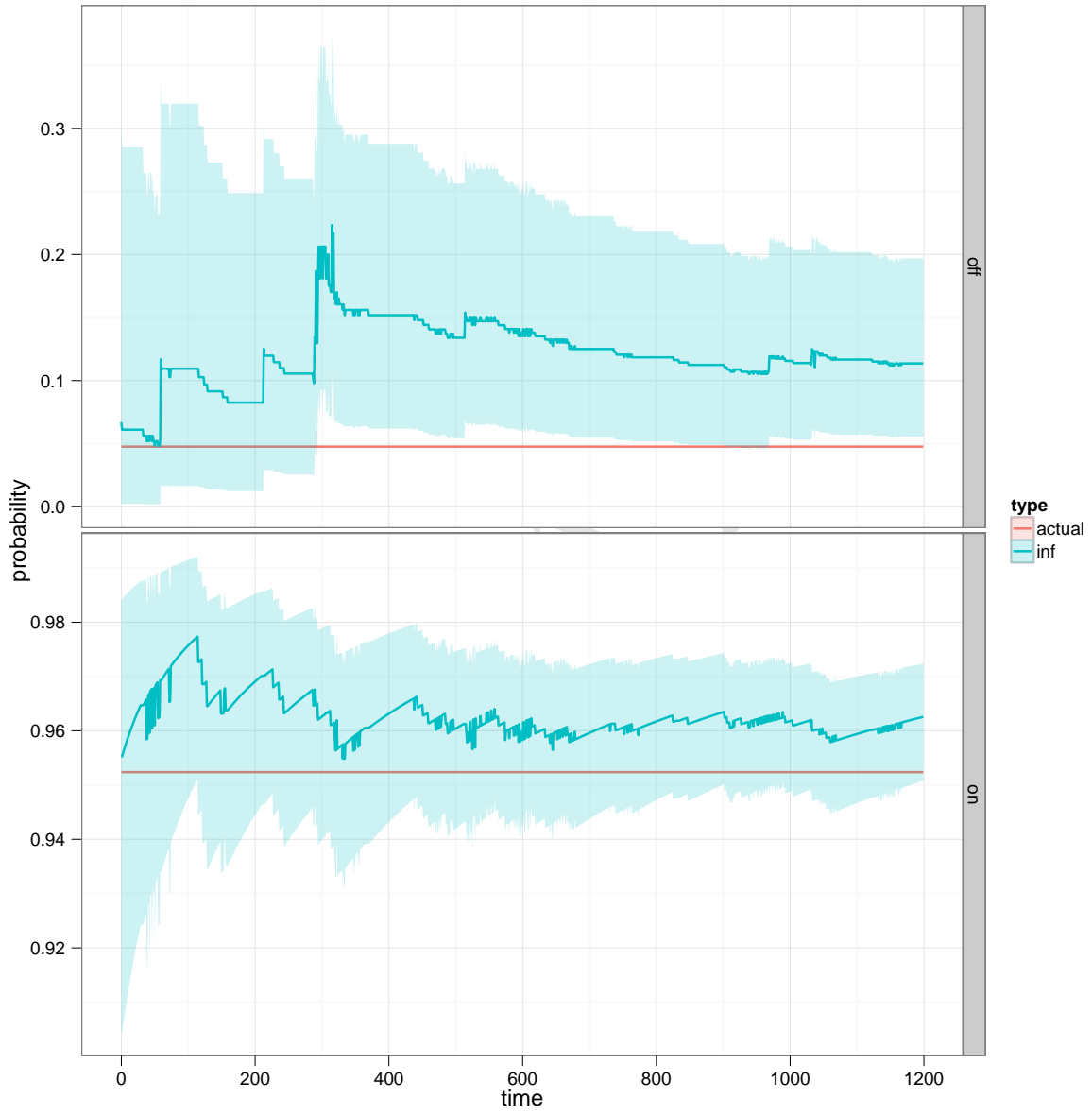
Figure 1: RMSE Comparisons

Figure 2: RMSE time series.

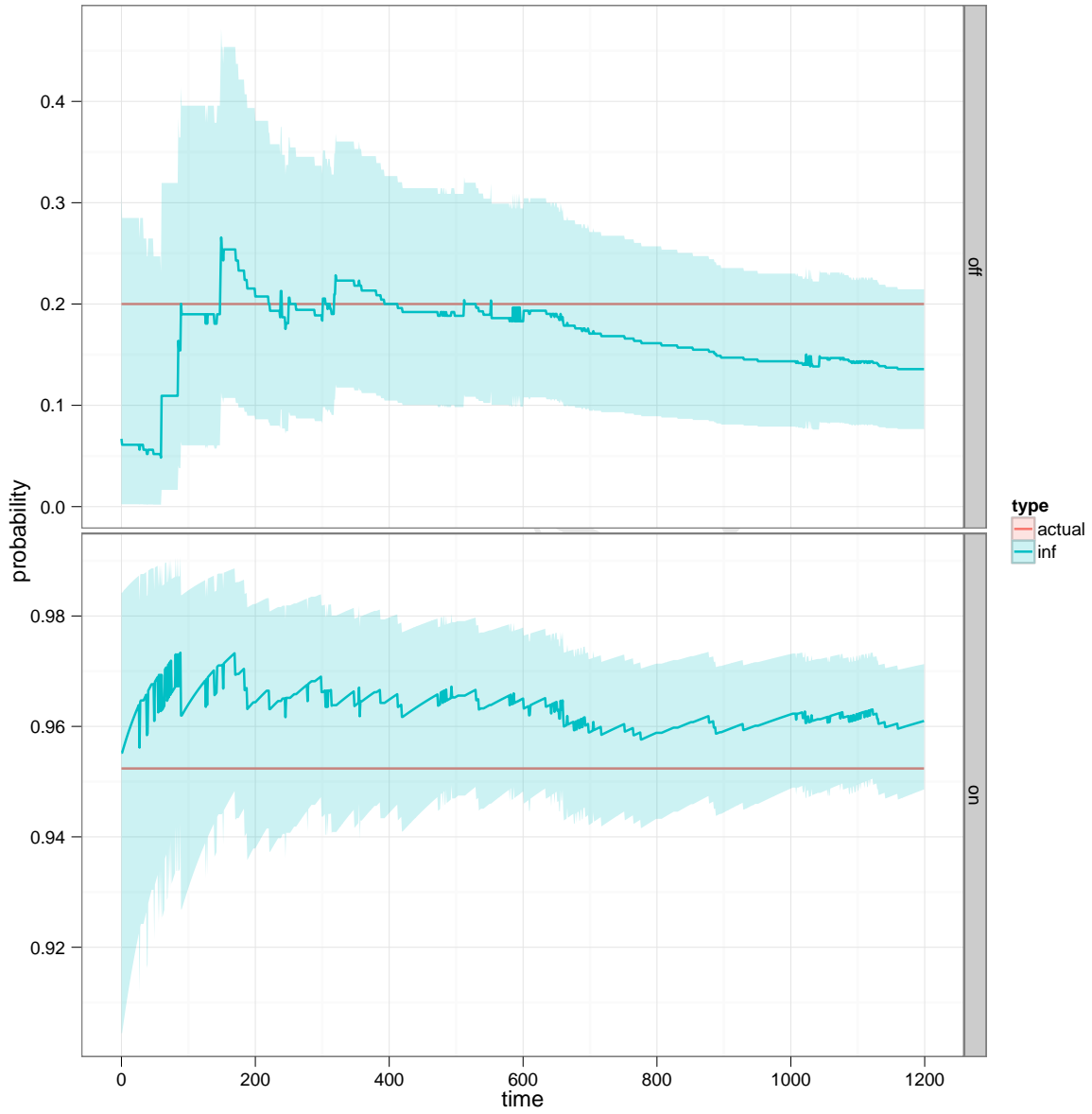Figure 3: Posterior Median 95% Credibility Intervals for π_{off}, π_{on}

Figure 4: Posterior Median 95% Credibility Intervals for π_{off}, π_{on}